Korean J. Chem. Eng., 35(8), 1626-1635 (2018)
DOI: 10.1007/s11814-018-0076-y

pISSN: 0256-1115
eISSN: 1975-7220

Comparative kinetic study of coal gasification with steam and CO_2 in molten blast furnace slags

Fan Yang, Qingbo Yu†, Huaqing Xie, Zongliang Zuo, Limin Hou, and Qin Qin

School of Metallurgy, Northeastern University, Shenyang, Liaoning 110819, P. R. China
(*Received 7 March 2018 • accepted 4 May 2018*)

Abstract−To make a comparison between coal gasification in molten blast furnace slag (MBFS) in different ambience and choose an appropriate agent to recover BF slag's waste heat entirely, coal gasification with steam and CO_2 in molten blast furnace slags was studied by isothermal thermo-gravimetric analysis. The effects of temperature and addition of MBFS were studied. Carbon conversion and reaction rate increased with increasing temperature and MBFS. Volumetric model (VM), shrinking core model (SCM), and diffusion model (DM) were applied to describe the coal gasification behavior of FX coal. The most appropriate model describing the coal gasification was SCM in steam ambience and VM in CO_2 ambience, respectively. The reaction rate constant k(T) in CO_2 ambience is greater than that in steam ambience, which means the gasification reactivity of coal in CO_2 ambience is better than that in steam ambience. BF slag can effectively reduce the activation energy E_A of coal gasification reaction in different ambiences. But, the difference of activation energies is not large in different ambiences. Based on the results of kinetic analysis including k(T) and E_A calculated by the established model, CO_2 was chosen to be the most appropriate agent.

Keywords: Coal Gasification, Molten Blast Furnace Slag, Heat Carrier, Kinetic Analysis, Isothermal Thermo-gravimetric

INTRODUCTION

Coal plays a vital role in China. However, the direct burning of coal easily brings a waste of resources, pollution of the environment and other issues. Therefore, the clean use of coal is particularly important. As we all know, many ways, like circulating fluidized bed boiler combustion (CFBC), ultra-supercritical coal-fired power generation (USC) and integrated coal gasification combined cycle (IGCC), are about clean use of coal. And among them, coal gasification, as a key technology for coal clean use, has attracted widespread attention and further research. Numerous studies on the intrinsic properties of coal like coal properties [1,2], coal pore structure [3-6], trace minerals in coal [7], and operating conditions like reaction temperature [8,9], heating rate [10,11] and pressure have been carried out.

Gasification involves a set of reactions, including the primary reaction like incomplete coal combustion (R1: $C+CO_2 \leftrightarrow 2CO$), steam decomposition reaction (R2: $C+H_2O \leftrightarrow CO+H_2$) and the secondary reaction like water-gas shift reaction (R3: $CO+H_2O \leftrightarrow CO_2+H_2$). The total reaction of coal gasification is endothermic. To date, most coal gasification technologies are self-heating, which means part of coal is burned to provide the corresponding heat for the coal gasification reaction.

To reduce fuel consumption, people began to look for other heat sources for coal gasification. As a by-product of blast furnaces from iron-making, blast furnace slag (BF slag) is usually a high-grade waste heat resource with tapping temperature about 1,673-1,723 K, which can be used as a heat carrier to provide the heat for coal gasification. Then the technology of coal gasification using BF slag as heat carrier was proposed and some scholars did some researches on coal gasification with blast furnace slag.

Part of these studies focused on the catalytic properties of blast furnace slag. The thermodynamic analysis, technology calculation and exergy analysis of synergistic gasification process of coal with BF slag were examined by Duan et al. [12-15]. It was found that the BF slag can act as a heat carrier and play a catalytic role at the same time in coal gasification reaction. The influences of reaction temperature, heating rate and slag/coal mass ratio on CO_2 gasification of coal with the BF slag were also studied by many researchers [16,17]. To obtain hydrogen-rich gas hydrogen-rich syngas, coal-steam reaction with the BF slag was studied by Duan [18]. The hydrogen fraction of syngas was higher than 63%. The catalytic mechanism of coal gasification using BF slag as heat carrier was schematically proposed [19].

Coal gasification using BF slag as heat carrier is also a way to recover the BF slag's waste heat by chemical method [20-24]. And some researchers focused on the recovery process and recovery efficiency of this method. For the purpose of recovering the waste heat of BF slag, a thermodynamic analysis of the synergistic coal-steam gasification process with BF slag as heat carrier was performed using the Gibbs free energy minimization approach by Duan [15], and the recovery efficiency theoretically can reach up to 83.08%. Li and Yu [25] proposed a new heat recovery system of BF slag that can effectively recover the waste heat of BF slag in different states (molten and solid states).

The gasification agent (steam, CO_2, O_2) has a great influence on coal gasification reaction [26-29]. And it may also have an important impact on the waste heat recovery of MBFS (a high-quality, high-

†To whom correspondence should be addressed.
E-mail: yuqb@smm.neu.edu.cn

Table 1. The proximate, ultimate analysis of coal samples

Coal	Proximate analysis (wt%)				Ash melting point (K)
	Moisture	Volatile matter	Fixed carbon	Ash	ST
	3.13	32.78	34.79	29.30	1603
	Ultimate analysis (wt%)				Heating value (MJ/Kg)
	C	H	O	N	S	26.65
	52.27	4.204	8.796	1.09	1.210	

Table 2. The chemical composition of BF slag

Slag	Chemical composition (%)						
	CaO	MgO	SiO_2	Al_2O_3	Fe_2O_3	TiO_2	Others
	41.21	8.22	8	11.05	2.78	0.35	2.01

temperature heat carrier). Therefore, it is significant to explore which gasification agent is more conducive to the gasification reaction in MBFS and propitious to recycle BF slag's waste heat fully. There is no such investigation about the comparison of gasification reaction in MBFS in different ambiences.

To this end, the CO_2 and steam gasification of Fuxin (FX) coal in MBFS was studied by thermo-gravimetric analyzer. And the influence of temperature and BF slag was clarified by isothermal thermo-gravimetric experiment method. The kinetics model of coal gasification was established under different atmosphere in MBFS by model fitting method. The kinetic parameters of coal gasification under different atmosphere were obtained. Finally, the most appropriate agent for the coal gasification with MBFS was chosen by comparing the results of kinetic analysis.

EXPERIMENTAL

1. Samples

FX coal from Fuxin City, Liaoning Province is known as a kind of low grade lignite, which is rich in reserves in China. The BF slag was obtained from a local iron and steel company. The coal and slag samples were dried at 353 K for 24 h, and then ground and sieved using standard sieves to obtain the average particles size about 74 μm.

The proximate analysis and ultimate analysis were performed using an automatic proximate analyzer and a CHNS/O Analyzer, respectively. At the same time, the chemical composition of slag was performed by X-ray fluoroscopy (XRF). The results of the proximate and ultimate analyses of coal samples and the chemical composition of slag are shown in Table 1 and Table 2.

2. Apparatus and Procedure

In this study, coal gasification in MBFS was performed in a thermo-gravimetric analyzer (SETSYS Evolution 18 TGA, sensitivity is 0.25 μg). The entire experimental system, shown schematically in Fig. 1, consists of a gas supply system, a steam generator, a thermo-gravimetric analyzer and a computer to record and analyze the experimental data.

First, coal samples of 8 mg (or mixture of BF slag and coal by specific proportion) were weighed by an analytical balance, which

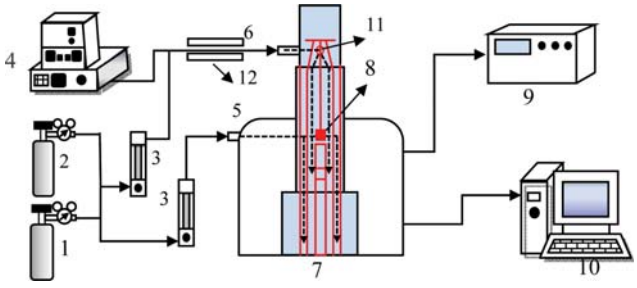

Fig. 1. The schematic of the SETSYS Evolution TGA experimental system.

1. Argon cylinder
2. CO_2 cylinder
3. Flow meter
4. Steam generator
5. Protective gas inlet
6. Gasification agent portal
7. SETSYS evolution 18 TGA
8. Crucible
9. Temperature controller
10. Computer
11. Balance
12. Insulation and preheating device

sensitivity was 0.1 mg, and then placed in a crucible with height of 4 mm and diameter of 6 mm. The crucible with samples was placed in the thermo-gravimetric analyzer, where the sample (coal or mixture of BF slag and coal by specific proportion) was heated to 1,273 K under atmospheric pressure with heating rate of 20 K min^{-1} and Argon flow rate of 30 ml min^{-1}, and then maintained at 1,273 K for 30 min to make sure the coal sample fully pyrolyzed. After pyrolysis, the analyzer was heated to design reaction temperature at heating rate of 20 K min^{-1} and argon flow rate of 30 ml min^{-1},

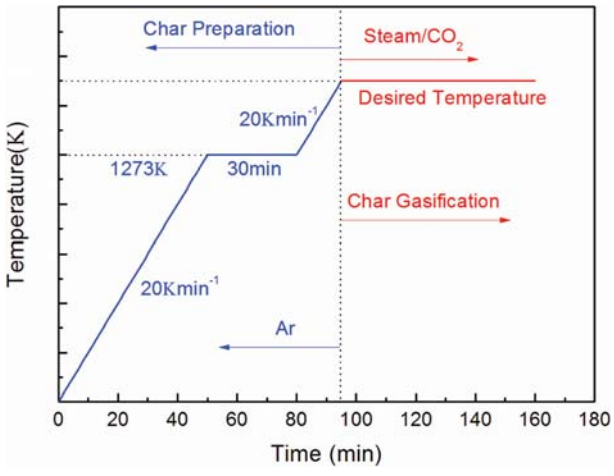

Fig. 2. The heating program of thermo-gravimetric analyzer.

Table 3. The experimental conditions

Temperature (K)	Slag/Coal mass ratio	Gasification agent	Pressure (KPa)	Carrier gas
1573	1 : 0			
1623	0 : 1	Steam/CO_2	101.325	Argon
1673	2 : 1			

after which argon was switched to gasification agent (steam or CO_2), and gasification reaction started. The whole experiment was under atmospheric pressure. Argon was used as carrier gas for steam and CO_2. The partial pressure of steam/CO_2 flow rate was 30.396 KPa. Steam generator and the transfer lines were maintained at 453 K and 423 K, respectively. Experimental data (mainly mass change of the sample over time) output was recorded by a computer. Heating procedure of the isothermal temperature experiments in detail is shown in Fig. 2. Design reaction temperatures for isothermal experiments were 1,573 K, 1,623 K and 1,673 K, respectively, which covers from the temperature of BF slag maintaining the molten state to the lowest discharge temperature of MBFS. To investigate the effect of BF slag on gasification reaction, all experiments were performed at two different slag/coal mass ratios: 0 : 1 and 2 : 1. Details of the experimental conditions are shown in Table 3.

3. Kinetic Models

During each experimental run, the weight of the sample and the time were saved automatically in a data log file. Considering the weight loss of BF slag, there are two expressions of carbon conversion (X) in this experiment. When the sample was coal only, carbon conversion (X) was calculated as follows:

$$X(t)=\frac{w_0-w_t}{w_0-w_{ash}}\times 100\% \tag{1}$$

where, w_0 is initial mass of the char, mg; w_t is mass of the char at a particular time, mg and w_{ash} is mass of the ash, mg. However, when the coal was gasified in the thermo-gravimetric analyzer with BF slag, the mass loss included both the mass change of coal and BF slag. To obtain the mass change of coal only, it is necessary to eliminate the influence of the mass change of BF slag. So, when the sample is mixture of coal and BF slag, carbon conversion (X) is calculated as:

$$X(t)=\left[\frac{(w_{c0}-w_{ct})}{(w_{c0}-w_{c\infty})}-\frac{(w_{s0}-w_{st})}{(w_{s0}-w_{s\infty})}\times\frac{m}{m+1}\right]\times(1+m)100\% \tag{2}$$

where, w_{c0} is initial mass of the char with BF slag, mg; w_{ct} is mass of the char with BF slag at a particular time, mg; $w_{c\infty}$ is final mass of the mixture of char and BF slag, mg; w_{s0} is initial mass of BF slag, mg; w_{st} is mass of BF slag at particular time, mg; $w_{s\infty}$ is final mass of BF slag at a termination of the program, mg; m is the ratio of BF slag to char. The w_{s0}, w_{st} and $w_{s\infty}$ is obtained by a blank run (only BF slag without coal).

According to the general rate law for gas-solid reaction, the reaction rate also can be expressed as the product of two independent functions of the independent variables' temperature and carbon conversion under isobaric consideration [28]. The apparent reaction rate is expressed as:

$$r=\frac{dX}{dt}=k(T)f(X) \tag{3}$$

where, k(T) is the rate constant. f(X) is a function of the solid surface and usually associated with the carbon conversion. The activation of char with oxidizing gas is a heterogeneous gas-solid reaction where pore structure and surface area of particle are changing due to the reaction. In the function, structural variations and other phenomena film mass transfer, pore diffusion, and chemical reaction have to be considered [16]. Therefore, many different mechanism functions were established. In this study, the single-step gas-solid kinetic models [30-34], volumetric model (VM), shrinking core model (SCM) and diffusion model (DM), were applied to the kinetics analysis. Details are shown in Table 4.

The partial pressure of gasification agent is constant in the gasification process in this study. Solving the first-order differential of Eq. (3), the gasification reaction time was a constant for a particular carbon conversion:

$$G(X)=\int_0^{X_c}\frac{dX}{f(X)}=\int_0^{t_c}k(T)dt=k(T)t \tag{4}$$

$$G(X)=k(T)t \tag{5}$$

where, G(X) is the integrated form of mechanism function. Details of the integrated form of mechanism function about these three models are shown in Table 4. On the right side of Eq. (5), k(T) is constant because of isothermal method. So, there should be linear relationship between G(X) and t. The linear correlation coefficient (R^2) could be calculated by linear fitting of the mechanism function. The most appropriate mechanism function f(X) was chosen by comparing the linear correlation coefficient (R^2) of different mechanism functions. The slope of G(X) (the integrated form of most appropriate mechanism function)-t curves at different reaction temperatures can be used to evaluate the reaction rate constant k(T). The model showing the best linear fitting was chosen as the most appropriate model.

Table 4. Differential and integral expressions of mechanism functions

Logogram	Model name	Differential form f(X)	Integral form G(X)
VM	Volumetric model	$2(1-X)[-\ln(1-X)]^{1/2}$	$[-\ln(1-X)]^{1/2}$
SCM	Shrinking core model	$2(1-X)^{1/2}$	$1-(1-X)^{1/2}$
DM1		$1/2\ X^{-1}$	X^2
DM2	Diffusion model	$[-\ln(1-X)]^{-1}$	$X+(1-X)\ln(1-X)$
DM3		$3/2(1+X)^{2/3}[(1+X)^{1/3}-1]^{-1}$	$[(1+X)^{1/3}-1]^2$

The rate constant (k(T)) is described by Arrhenius equation; the empirical formula is given by:

$$k(T) = k_0 e^{-\frac{E_A}{RT}} \quad (6)$$

where, k_0 is pre-exponential factor, min^{-1}; E_A is the activation energy, $kJmol^{-1}$; R is the ideal gas law constant, $kJmol^{-1}K^{-1}$, and T is the absolute temperature, K.

By taking the logarithm of Eq. (6), Eq. (7) could be obtained:

$$\ln K = \ln k_0 - \frac{E_A}{R} \times \frac{1}{T} \quad (7)$$

In this work, linearized or linear regression of logarithm expression was used to obtain E_A and k_0. E_A and k_0 were estimated through the correlation of data (K and T) at different reaction temperatures in an alternative form of Arrhenius equation.

RESULTS AND DISCUSSION

1. Effects of the Temperature and MBFS on Carbon Conversion

As shown in Fig. 3(a), carbon conversion increases with time. Within the same reaction time, carbon conversion increases with temperature in steam ambience and experiment temperature range, especially from 1,623 K to 1,673 K. Fig. 3(b) shows that carbon conversion increases steeply during first 20 min and then gradually slows, and seems to reach a plateau. Within the same reaction time, carbon conversion of FX coal at 1,573 K is higher than that at 1,623 K and 1,673 K at the first 10 min in CO_2 ambience without MBFS. Then, it gradually increases with temperature after 20 min. This is because these reaction temperatures are relatively close to the FX coal ash melting point temperature, which is 1,603 K, as shown in Table 1. The coal gasification process is affected by the ash melting state of coal. This phenomenon was also found in Liu's research [35,36], that the reaction rate of the char with low fusion temperature leveled off, or even decreased a little as temperature increased. It indicates that the reactivity of coal is affected by the ash fusion temperature.

As shown in Fig. 3(a) and Fig. 3(b), because of the addition of BF slag, carbon conversion at the same temperature increases and the completion time of gasification reaction in different ambience is shortened. It indicates that the MBFS has a positive effect on coal gasification. As can be seen from Table 2, BF slag contains a large amount of CaO, about 41%, while calcium oxide is an active ingredient in calcium-containing ores and plays an important cat-

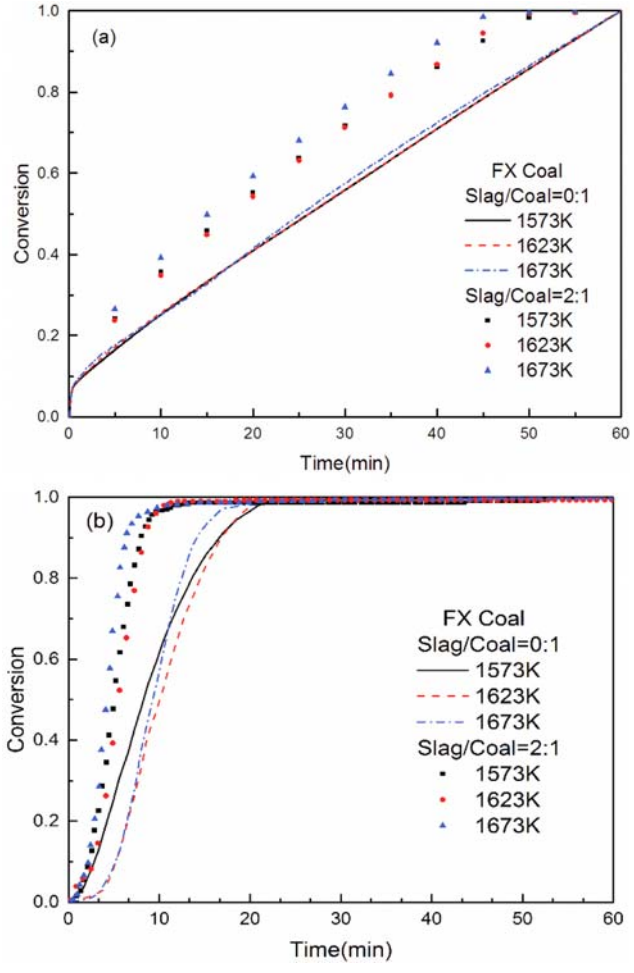

Fig. 3. Carbon conversion versus time curves for the gasification of FX coal under (a) Steam and (b) CO_2.

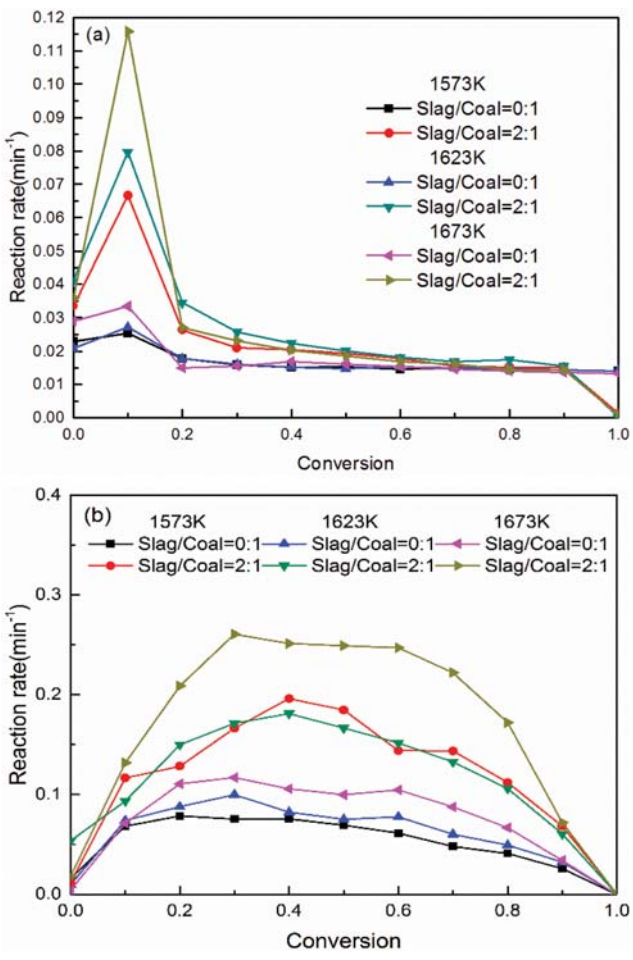

Fig. 4. Reaction rate versus carbon conversion curves for the gasification of FX coal under (a) Steam and (b) CO_2.

alytic role in coal gasification [37]. Due to the addition of MBFS, some specific reactions occurred. It helps to improve carbon conversion and reaction rate [14,38,39].

$CaO+1/2O_2 \leftrightarrow CaO_2$
$CaO_2+C \leftrightarrow CaO+CO$

Besides, BF slag contains other elements like alkali earth metal Mg and transition metal Fe, which have been proved to have a catalytic effect on coal gasification by many researchers [40,41].

Comparing the carbon conversion curves in different ambience, the completion time of the reaction in CO_2 ambience is shorter than that in steam ambience. Fig. 4 shows that the CO_2 gasification rate of coal is higher than the corresponding steam gasification rate. It indicates that the gasification reactivity in CO_2 ambience is better than that in steam ambience in the higher temperature range. This is contrary to the common understanding. Because, in general, the reactivity of coal gasification in steam ambience is higher than that in CO_2 ambience. Most of this conclusion is based on the results obtained in the temperature range of 973 K to 1,373 K [26,27,29,37]. Therefore, it is possible that high temperature may be one of the reasons for better gasification reactivity of coal-CO_2 gasification than the corresponding steam-coal gasification. Some published researches imply similar results [42,43]. In Ren's research [42], the gasification reactivity of five kinds of low-rank coal, a kind of mid-rank coal and three kinds of high-rank coal were investigated in the temperature range 1,273-1,873 K and different ambience under atmospheric pressure. For low-rank coals and mid-rank coals, the CO_2 gasification rate is higher than the steam reaction rate, which is consistent with our results. But for some kinds of high-rank coals and pet coke, the steam gasification rate is still higher than the CO_2 reaction rate. Therefore, the coal properties may be another reason for better gasification reactivity of coal-CO_2 gasification than the corresponding steam-coal gasification. The properties including coal structure and AAEMs (alkali and alkaline earth metals) in coals especially the catalytic effect of AAEMs should be a key factor. It has been reported that the AAEMs is more active for the CO_2-gasification than that for the steam-gasification [44]. The low-rank coal contains relatively high amounts of AAEMs, while the high-rank coal contains little AAEMs. With the aid of AAEMs the gasification reactivity of coal in CO_2 may be higher than that in steam at high temperature.

Table 5. Gibbs free energy of R1, R2 and R3 at different temperature

T(K)	Gibbs free energy (kJmol^{-1})			
	$\Delta G_{m\text{-}R1}$	$\Delta G_{m\text{-}R2}$	$\Delta G_{m\text{-}R3}$	$\Delta G_{m\text{-}R}-\Delta G_{m\text{-}R2}$
1073	−17.526	−18.041	−0.515	0.515
1173	−34.943	−32.371	2.571	−2.572
1273	−52.268	−46.693	5.576	−5.575
1373	−69.506	−60.998	8.508	−8.508
1473	−86.660	−75.283	11.377	−11.377
1573	−103.734	−89.544	14.190	−14.19
1673	−120.732	−103.778	16.953	−16.954
1773	−137.656	−117.984	19.672	−19.672

This phenomenon can be explained from the thermodynamic point of view. Table 5 lists the Gibbs free energy of the main reactions of CO_2 and steam gasification (R1 and R2) and water-gas shift reaction (R3). The Gibbs free energy of water-gas shift reaction is greater than 0 at a temperature above 1,173 K, which means the water-gas reaction does not occur when the temperature exceeds 1,173 K. It shows that the coal-CO_2 gasification reaction is more favorable than coal-steam gasification reaction in the higher temperature range.

2. Effects of the Temperature and Slag/Coal Mole Ratio on Reaction Rate

The reaction rate is obtained by Eq. (3) based on the carbon conversion data. The reaction rate curves for the coal-steam and coal-CO_2 gasification at different temperature conditions and slag/coal mass ratios are shown in Fig. 4, respectively. Fig. 4(a) shows that the reaction rate increases sharply and reaches the maximum value at conversion of 0-10%, and then decreases at conversion of 10-20%. The reaction rate peak occurs at the carbon conversion of 0.1. The peak value increases with temperature. Fig. 4(b) shows that the reaction rate increases first and then decreases in CO_2 ambience. Simultaneously, because of the addition of BF slag, reaction rate is improved in both ambiences.

Comparing the reaction rate versus carbon conversion curves of FX coal gasification in different ambience, the main change of reaction rate occurs at a narrow conversion range of 0-20%, but, in CO_2 ambience, the main change of reaction rate occurs at a wide conversion range of 0-100%. In other words, the reaction rate varied more gently in CO_2 ambience than that in steam ambience. But, the reaction rate of FX coal gasification in CO_2 ambience is greater than that in steam ambience. It means that the gasification reactivity in CO_2 ambience is better than that in steam ambience. The reason has been discussed in the previous section.

3. Modeling and Kinetic Parameter Calculation

Various mechanism functions (as shown in Table 4) are used to fit the experiment results above. Based on Eqs. (3), (4) and (5), the most appropriate mechanism function f(X) can be obtained by analyzing the linear relationship between G(X) and t. Therefore, the linear correlation coefficient (R^2) in all experiment conditions was adopted in kinetic analysis to find an appropriate mechanism function to describe coal gasification in different ambience. The reaction rate constants k(T) is obtained by calculating the slope of G(X) (the integrated form of most appropriate mechanism function)-t curves at reaction temperatures. Based on the established mechanism function, the reaction activation energy (E_A) and pre-exponential factor (k_0) will be obtained by Eqs. (6) and (7).

The R^2 for all experiment conditions in different ambience are shown in Fig. 5 and Fig. 6. It can be seen from Fig. 5 that SCM is better than other reaction model in steam ambience. At the meanwhile, as can be seen from Fig. 6, VM is better than other reaction model in CO_2 ambience.

It can be seen from Table 6 that k(T) increases with temperature. It also indicates that the addition of BF slag increases the reaction rate constants k(T) effectively. Comparing the reaction rate constants k(T) in different ambience, the reaction rate constant k(T) in CO_2 ambience is greater than that in steam ambience. It is consistent with the changes of reaction rate with temperature,

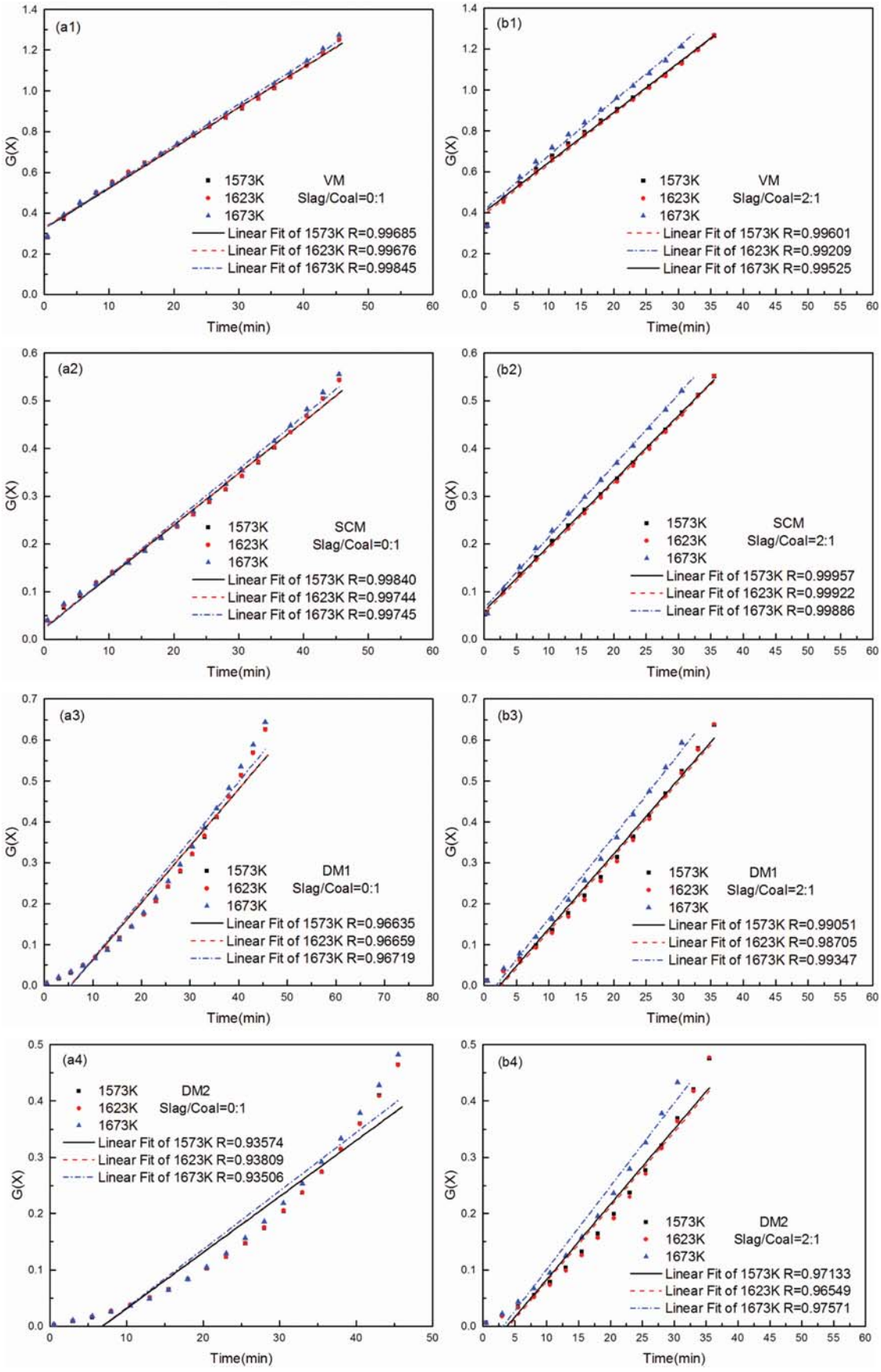

Fig. 5. The linearized expressions of different models for FX coal in steam ambience.

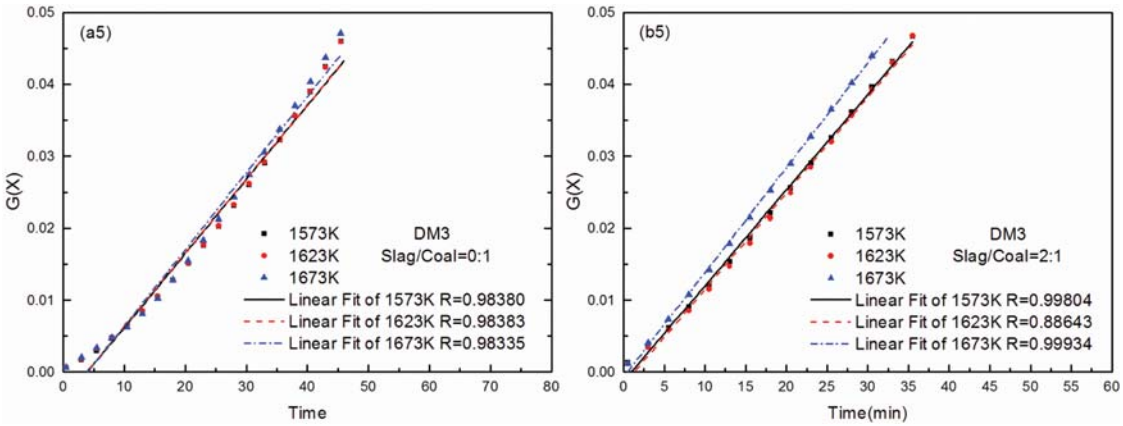

Fig. 5. Continued.

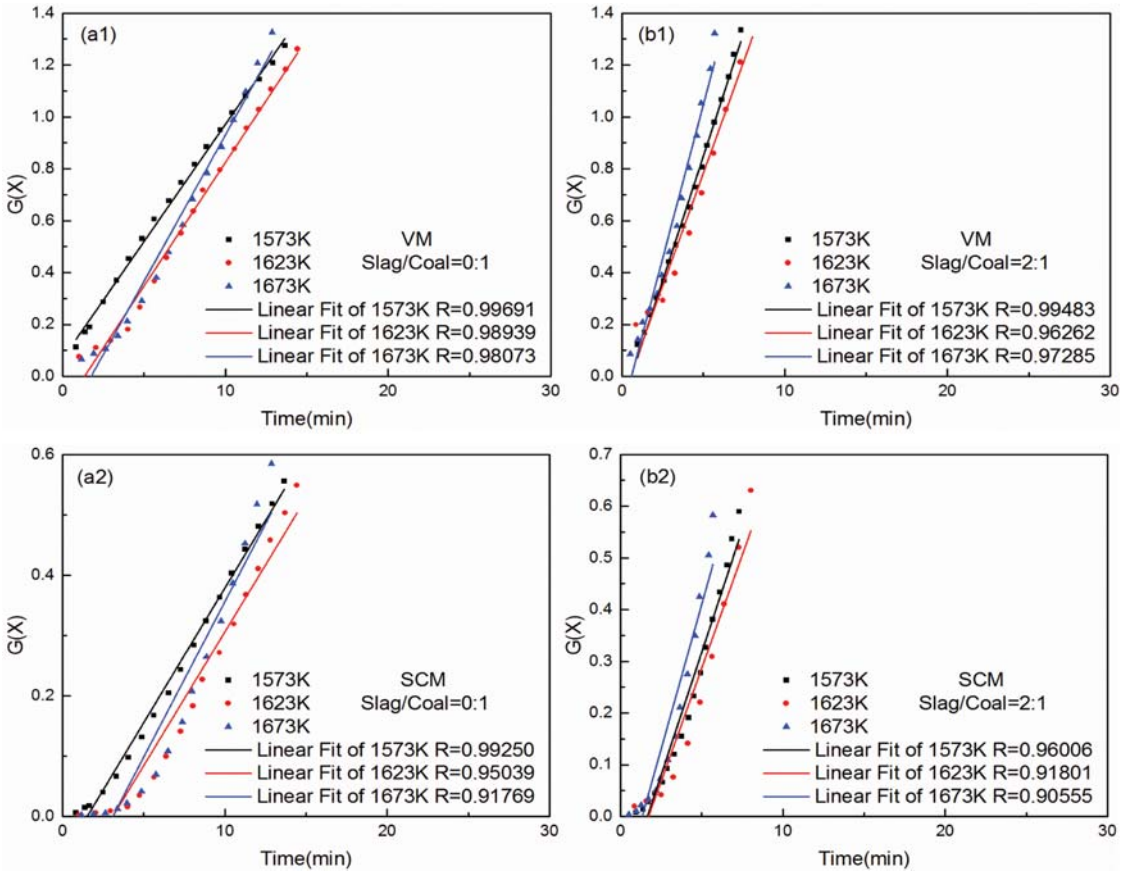

Fig. 6. The linearized expressions of different models for FX coal in CO_2 ambience.

ambience and Slag/Coal mass ratio, and shows that the gasification reactivity in CO_2 ambience is better than that in steam ambience.

The reaction rate equation (including E_A and k_0) of coal gasification was established and shown in Table 7. It can be seen from Table 7 that the activation energy of FX coal reduced from 46.1 to 19.4 kJmol^{-1} in steam ambience and from 48.3 to 42.7 kJmol^{-1} in CO_2 ambience because of the addition of BF slag. It indicates that gasification reactions occur more easily in MBFS. No matter if there is MBFS or not, the difference of activation energies are not large in different ambience. Therefore, CO_2 is the most appropriate agent by comparing the results of kinetic analysis including reaction rate constants k(T) and the activation energy E_A calculated by the established model.

The activation energy E_A values reduce accompanied by a simultaneous reduce of the pre-exponential factor k_0 by addition of MBFS. The corresponding change of E_A, k_0 is so-called "compensation effect" [45].

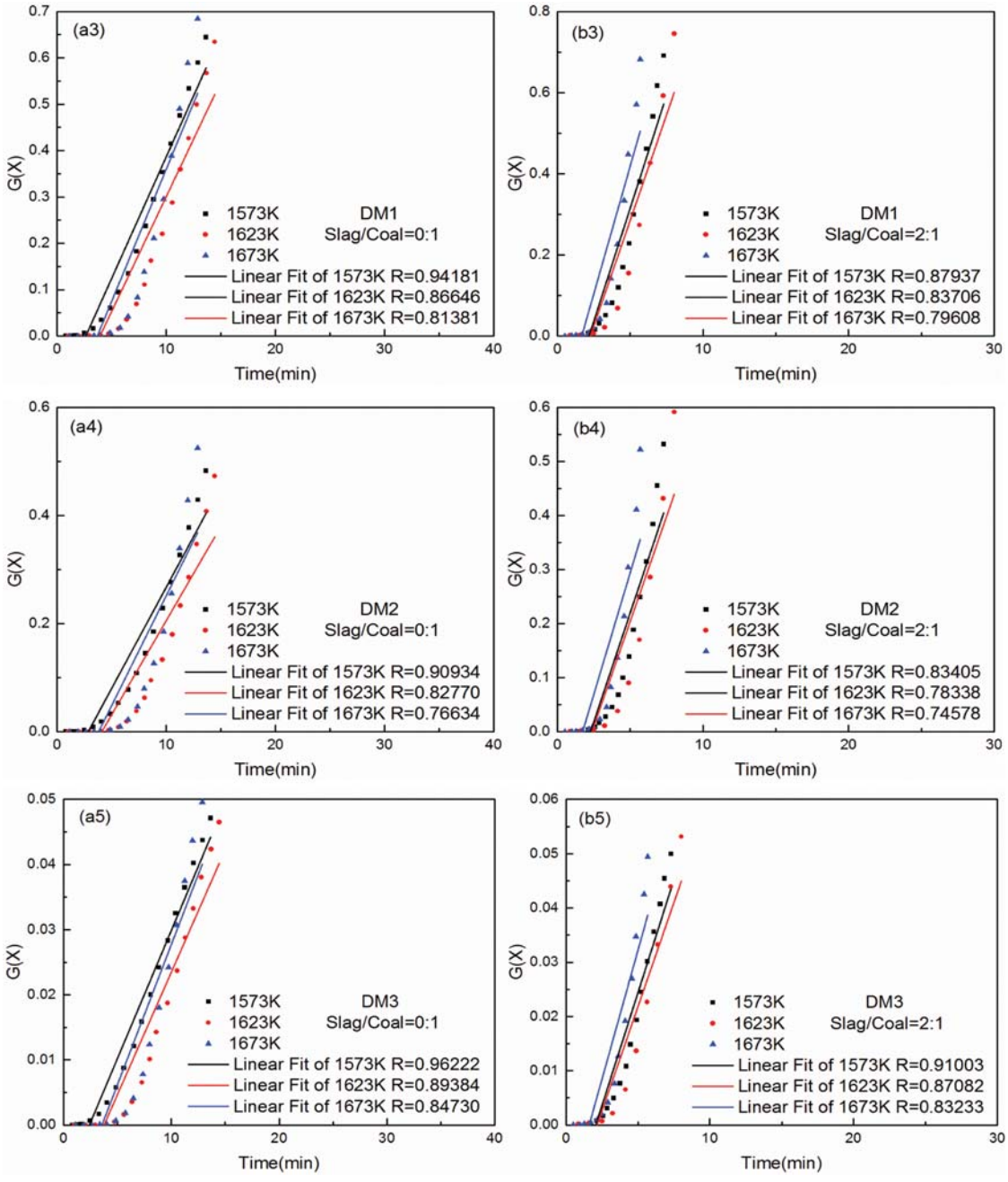

Fig. 6. Continued.

Table 6. The reaction rate constants in different temperature and slag/coal mass ratio conditions

Steam				CO_2			
Slag/Coal	1573 K	1623 K	1673 K	Slag/Coal	1573 K	1623 K	1673 K
0 : 1	0.00976	0.01088	0.01205	0 : 1	0.08848	0.09915	0.11035
2 : 1	0.01355	0.01419	0.01481	2 : 1	0.09882	0.10928	0.12013

Comparisons between the experimental data and calculated values got by the established model have been shown in Fig. 8. It is shown that the calculated values of the established model have a high consistency with the experimental data when the gasification reaction occurs in the molten blast furnace slags.

CONCLUSION

A kinetic study of steam gasification of FX coal with MBFS as heat carrier was performed by isothermal thermo-gravimetric experiment. The results demonstrated that BFS presented an important

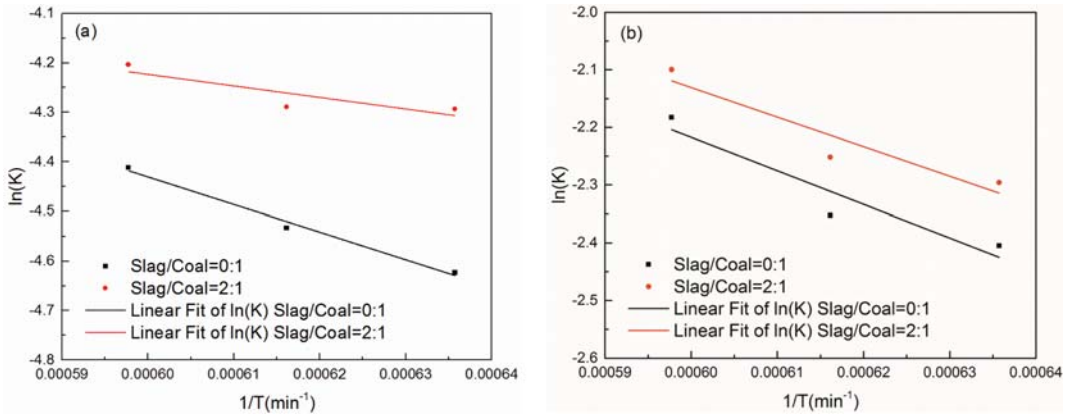

Fig. 7. Linear fitting for the calculation of the activation energy and pre-exponential factor with the appropriate mechanism function: (a) Steam gasification; (b) CO_2 gasification.

Table 7. The established model and kinetic parameters

Gasification agent	Steam		CO_2	
Slag/Coal	0 : 1	2 : 1	0 : 1	2 : 1
The established model	SCM $\frac{dx}{dt}=2k_0e^{\frac{-E_A}{RT}}(1-x)^{1/2}$		VM $\frac{dx}{dt}=2k_0e^{\frac{-E_A}{RT}}(1-x)[-\ln(1-x)]^{1/2}$	
E_A, kJmol^{-1}	46.1	19.4	48.3	42.7
k_0, min^{-1}	0.332	0.059	3.559	2.590

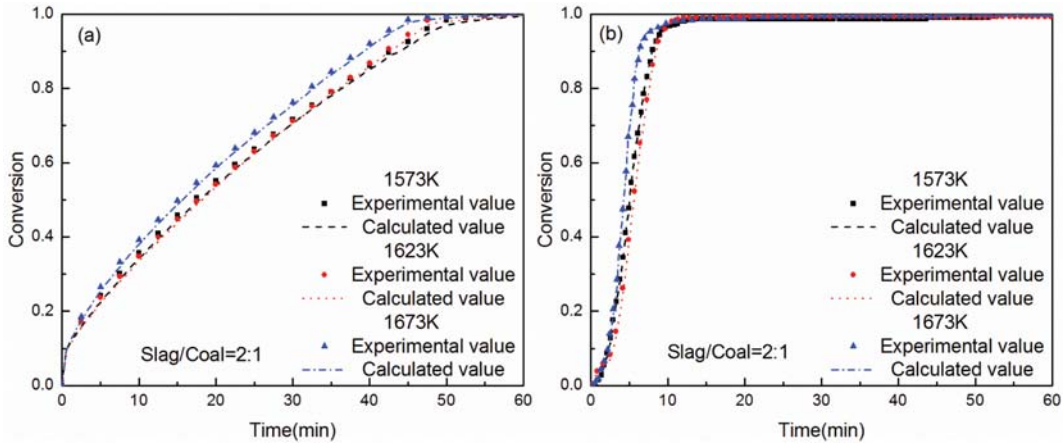

Fig. 8. Comparison between experimental data and calculate values by the established model: (a) Steam gasification; (b) CO_2 gasification.

role in coal gasification, not only as a heat carrier but also an effective catalyst. The carbon conversion and reaction rate increased with increasing temperature and addition of MBFS. The most appropriate model describing the coal gasification was SCM in steam ambience and VM in CO_2 ambience, respectively. The reaction rate constant k(T) in CO_2 ambience is greater than that in steam ambience. It indicated that gasification reactivity in CO_2 ambience is better than that in steam ambience. The addition of BF slag effectively reduced the activation energy of coal gasification reaction in different ambiences. The difference of activation energies was not large in different ambience. Therefore, CO_2 is the most appropriate agent, which is determined by the results of kinetic analysis including reaction rate constants k(T) and the activation energy E_A calculated by the established model.

ACKNOWLEDGEMENT

This research was supported by the Major State Research Development Program of China (2017YFB0603603), the National Natural Science Foundation of China (51604077, 51704071), the Fundamental Research Fund for the Central Universities (N170204016) and the China Postdoctoral Science Foundation (2017M621148).

NOMENCLATURE

Symbols

E_A : the activation energy [kJmol^{-1}]
f(x) : differential mechanism function
k(T) : rate constant is the function of temperature
k_0 : pre-exponential factor [min^{-1}]
m : mass ratio of BF slag to char
r : reaction rate [min^{-1}]
R : ideal gas law constant [kJmol^{-1}K^{-1}]
R^2 : the coefficient of determination
T : the absolute temperature [K]
w_0 : initial mass of the char [mg]
w_t : mass of the char at a particular time [mg]
w_{ash} : mass of the ash [mg]
w_{c0} : initial mass of the char with BF slag [mg]
w_{ct} : mass of the char with BF slag at a particular time [mg]
$w_{c\infty}$: final mass of the mixture of char and BF slag [mg]
w_{s0} : final mass of BF slag at a termination of the program [mg]
w_{st} : w_{st} is mass of BF slag at particular time [mg]
$w_{s\infty}$: final mass of BF slag at a termination of the program [mg]
X : carbon conversion [%]

REFERENCES

1. A. Molina and F. Mondragon, *Fuel*, **77**, 1831 (1998).
2. T. Takarada, Y. Tamai and A. Tomita, *Fuel*, **64**, 1438 (1985).
3. F. J. Maldonado-Hódar, J. Rivera-Utrilla and A. M. Mastral-Lamarca, *Fuel*, **74**, 823 (1995).
4. B. Feng and S. K. Bhatia, *Carbon*, **41**, 507 (2003).
5. Y. Niu, S. Wang, Y. Gong and S. e. Hui, *Energy Procedia*, **142**, 1635 (2017).
6. S. Zhu, Y. Bai, K. Luo, C. Hao, W. Bao and F. Li, *J. Anal. Appl. Pyrol.*, **128**, 13 (2017).
7. Y. Sekine, K. Ishikawa, E. Kikuchi and M. Matsukata, *Energy Fuel*, **19**, 326 (2005).
8. Q. Sun, W. Li, H. Chen and B. Li, *Fuel*, **83**, 1787 (2004).
9. J. Xi, J. Liang, X. Sheng, L. Shi and S. Li, *J. Anal. Appl. Pyrol.*, **117**, 228 (2016).
10. R.-L. Du, K. Wu, D.-A. Xu, C.-Y. Chao, L. Zhang and X.-D. Du, *Fuel Process Technol.*, **148**, 295 (2016).
11. S. Niksa, L. Heyd, W. Russel and D. Saville, Symposium (International) on Combustion, Elsevier, 1445 (1985).
12. W. Duan, Q. Yu, Z. Zuo, Q. Qin, P. Li and J. Liu, *Energy Convers. Manage.*, **87**, 185 (2014).
13. W. Duan, Q. Yu, H. Xie, Q. Qin and Z. Zuo, *Int. J. Hydrogen Energy*, **39**, 11611 (2014).
14. W. Duan, Q. Yu, H. Xie, J. Liu, K. Wang, Q. Qin and Z. Han, *Int. J. Hydrogen Energy*, **41**, 1502 (2016).
15. W. Duan, Q. Yu, K. Wang, Q. Qin, L. Hou, X. Yao and T. Wu, *Energy Convers. Manage.*, **100**, 30 (2015).
16. P. Li, Q. Yu, Q. Qin and W. Lei, *Ind. Eng. Chem. Res.*, **51**, 15872 (2012).
17. P. Li, Q. Yu, H. Xie, Q. Qin and K. Wang, *Energy Fuel*, **27**, 4810 (2013).
18. W. Duan, Q. Yu, T. Wu, F. Yang and Q. Qin, *Int. J. Hydrogen Energy*, **41**, 18995 (2016).
19. W. Duan, Q. Yu, J. Liu, T. Wu, F. Yang and Q. Qin, *Energy*, **111**, 859 (2016).
20. E. Kasai, T. Kitajima, T. Akiyama, J. Yagi and F. Saito, *ISIJ Int.*, **37**, 1031 (1997).
21. Y. Qin, X. Lv, C. Bai, G. Qiu and P. Chen, *Jom-us.*, **64**, 997 (2012).
22. H. Zhang, H. Wang, X. Zhu, Y.-J. Qiu, K. Li, R. Chen and Q. Liao, *Appl. Energy*, **112**, 956 (2013).
23. M. Barati, S. Esfahani and T. Utigard, *Energy*, **36**, 5440 (2011).
24. Y. Sun, Z. Zhang, L. Liu and X. Wang, *Energies*, **8**, 1917 (2015).
25. P. Li, Q. Qin, Q. B. Yu and W. Y. Du, Advanced Materials Research, Trans Tech Publ., 2347 (2010).
26. J. Tanner and S. Bhattacharya, *Chem. Eng. J.*, **285**, 331 (2016).
27. Y. Wang and D. A. Bell, *Fuel*, **187**, 94 (2017).
28. A. Gomez and N. Mahinpey, *Chem. Eng. Res. Des.*, **95**, 346 (2015).
29. K. Jayaraman, I. Gökalp and S. Jeyakumar, *Appl. Therm. Eng.*, **110**, 991 (2017).
30. J. H. Zou, Z. J. Zhou, F. C. Wang, W. Zhang, Z. H. Dai, H. F. Liu and Z. H. Yu, *Chem. Eng. Process.: Process. Intensification*, **46**, 630 (2007).
31. R. Silbermann, A. Gomez, I. Gates and N. Mahinpey, *Ind. Eng. Chem. Res.*, **52**, 14787 (2013).
32. S. K. Bhatia and D. Perlmutter, *AIChE J.*, **26**, 379 (1980).
33. M. F. Irfan, M. R. Usman and K. Kusakabe, *Energy*, **36**, 12 (2011).
34. B. Janković, B. Adnađević and J. Jovanović, *Thermochim. Acta*, **452**, 106 (2007).
35. H. Liu, C. Luo, S. Kato, S. Uemiya, M. Kaneko and T. Kojima, *Fuel Process. Technol.*, **87**, 775 (2006).
36. H. Liu, C. Luo, M. Toyota, S. Uemiya and T. Kojima, *Fuel Process. Technol.*, **87**, 769 (2006).
37. M. Gao, Z. Yang, Y. Wang, Y. Bai, F. Li and K. Xie, *Fuel*, **189**, 312 (2017).
38. Y. Sun, J. Nakano, L. Liu, X. Wang and Z. Zhang, *Sci. Rep-uk.*, **5**, 11436 (2015).
39. Y. Sun, Z. Zhang, L. Liu and X. Wang, *Bioresour. Technol.*, **181**, 174 (2015).
40. M. Kannan and G. Richards, *Fuel*, **69**, 747 (1990).
41. D. W. McKee, *Carbon*, **12**, 453 (1974).
42. L. Ren, J. Yang, F. Gao and J. Yan, *Energy Fuel*, **27**, 5054 (2013).
43. H. Liu, H. Zhu, M. Kaneko, S. Kato and T. Kojima, *Energy Fuel*, **24**, 68 (2010).
44. D. P. Ye, J. B. Agnew and D. K. Zhang, *Fuel*, **77**, 1209 (1998).
45. A. R. Pande, *Fuel*, **71**, 1299 (1992).